Laser cooling of ions stored in a Penning trap: A phase-space picture

G. Zs. K. Horvath* and R. C. Thompson

The Blackett Laboratory, Imperial College, Prince Consort Road, London SW7 2BZ, England

We present a phase-space picture of laser cooling of the radial motion of ions in a Penning trap. This picture enables a particularly simple derivation of the condition for simultaneous cooling of all degrees of freedom of a single ion to be obtained. It also allows a physically intuitive approach to be taken to the cooling process. Using this approach, we discuss different aspects of the cooling of a single ion in a Penning trap, including the formation of ''trapped'' states where the steady-state motion amplitude is nonzero for either the magnetron or modified cyclotron motion. We use an analytical approach where the approximation of small-amplitude motions can be made, and we use numerical calculations for larger-amplitude motions. The best procedure to use for effective laser cooling is derived. A similar approach is then used to treat the laser cooling of two ions in the Penning trap. We show that the use of the phase-space approach allows new insights into many aspects of the laser-cooling process to be gained, and we indicate how these insights may be applied in experimental investigations. [S1050-2947(99)02406-3]

PACS number(s): 32.80.Pj

I. INTRODUCTION

It is now over 30 years since the first concrete proposals for laser cooling of atomic particles were made by Wineland and Dehmelt [1] and Hänsch and Schawlow [2]. One of the first demonstrations of laser cooling was performed on magnesium ions held in a Penning trap [3]. Laser cooling is now widely used in both Paul and Penning traps. Although the general cooling mechanism involved, that is, Doppler cooling, is the same for both traps, the actual dynamical properties of the trapped particles lead to important differences in the cooling process.

In this paper we will consider the laser cooling of small numbers of particles confined in a Penning trap. We concentrate on the case where the laser cooling beam is parallel to the radial plane (perpendicular laser cooling). In doing this we do not cool directly the axial motion. However, we will see that the results obtained in this case remain qualitatively valid when the laser is oriented at an angle with respect to the trap axis, in which case the axial motion can also be cooled. The motion is considered in the classical limit and the interaction with the laser is modeled semiclassically. We limit ourselves to the study of steady states of the ions' motion, although the theory presented here could easily be extended to calculate, for example, cooling rates or mean scattering rates.

We study first the laser cooling of a single ion and we calculate the conditions that the laser detuning and offset (in the radial plane) must satisfy in order to laser cool an ion to its minimum kinetic energy. In the following sections, we extend our calculations to the two-ion crystal and then to larger clouds. Most studies on laser cooling in the Penning trap have concentrated on calculating the ions' temperature rather than the cooling conditions. This is partly due to the complexity of the problem which involves many degrees of

freedom: three ion oscillation frequencies and motional amplitudes, beam waist size, laser power, beam offsets and orientation, and laser detuning. All these parameters will affect differently the cooling of the three degrees of freedom of a single ion.

To date work done on laser cooling in the Penning trap has dealt with either a single ion or a large cloud whose steady-state temperature was analyzed statistically. The condition for laser cooling for a single ion was studied numerically by Thompson and Wilson [4,5]. The steady-state temperature of a single ion was calculated analytically by Itano and Wineland [6]. They also calculated, numerically this time, the steady-state temperature of a large cloud subjected to laser cooling, which was successfully verified experimentally [7]. However, this approach neglected the effect of the torque applied by the laser beam on the cloud.

The usual picture for laser cooling is that if the laser is detuned below resonance and offset from the trap center on the side where the magnetron motion recedes from the laser, both cyclotron and magnetron degrees of freedom will be cooled. However, Wilson has shown (in the case of a single ion) the presence of nontrivial steady states of the magnetron motion (that is, steady motion with a large magnetron radius) which seems to be supported by experimental evidence [5].

In this paper we find what conditions the laser detuning and offset have to satisfy in order to simultaneously laser cool both radial degrees of freedom for given oscillation frequencies, beam waist, and laser power. In addition we show that the nontrivial steady states are stable and find the conditions under which they exist.

II. COOLING OF A SINGLE ION

A. Motion of an ion in a Penning trap

The motion of an ion stored in a Penning trap has been extensively treated previously [8,9]. Let us briefly summarize the relevant features. Trapping in the Penning trap is achieved with a quadratic electric potential:

---

*Present address: Institut d'Optique, Boîte Postale 147, F-91403 Orsay Cedex, France.
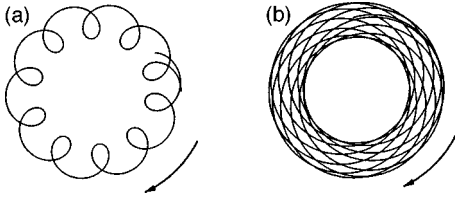
FIG. 1. Radial orbit of a single particle in quadrupole traps. (a) Penning trap with a magnetron radius larger than the modified cyclotron radius. (b) Same as (a) but with the magnetron radius smaller than the modified cyclotron radius.

$$\phi(r,z) = \frac{U_0}{R_0^2}(2z^2 - r^2), \tag{1}$$

where $r^2 = x^2 + y^2$ and $R_0^2 = r_0^2 + 2z_0^2$, $2r_0$ is the diameter of the trap ring electrode, $2z_0$ is the separation of the endcap electrodes, and U_0 is a potential applied between the endcap electrodes and the ring electrode. For trapping positively charged particles, U_0 must be positive. This potential then has a saddle point at the trap center, with a minimum in the axial direction and a maximum in the radial plane. The particle will therefore be confined in the axial direction but attracted towards the ring electrode. A static homogeneous magnetic field B along the z axis provides radial confinement by forcing the particle's orbit into epicyclic orbits in the radial plane (see Fig. 1). The equation of motion for a single trapped ion of charge q and mass m is easily solved to give the following solutions:

$$x(t) = r_+ \cos(\omega_+ t + \varphi_+) + r_- \cos(\omega_- t + \varphi_-), \tag{2a}$$

$$y(t) = -r_+ \sin(\omega_+ t + \varphi_+) - r_- \sin(\omega_- t + \varphi_-), \tag{2b}$$

$$z(t) = r_z \cos(\omega_z t + \varphi_z), \tag{2c}$$

where r_+, r_-, r_z are the amplitudes of the various degrees of freedom, $\varphi_+, \varphi_-, \varphi_z$ their initial phases, and where we have defined

$$\omega_+ = \tfrac{1}{2}(\omega_c + \omega_1) \quad \text{modified cyloctron frequency,}$$

$$\omega_- = \tfrac{1}{2}(\omega_c - \omega_1) \quad \text{magnetron frequency,}$$

$$\omega_z^2 = \frac{4qU_0}{mR_0^2} \quad \text{axial frequency,}$$

with

$$\omega_c = \frac{qB}{m} \quad \text{cyloctron frequency,}$$

$$\omega_1^2 = \omega_c^2 - 2\omega_z^2.$$

The axial motion is simple harmonic with frequency ω_z. In the radial plane the motion consists of a superposition of two circular motions which results in an epicyclic orbit (Fig. 1). The modified cyclotron frequency, ω_+, mainly due to the effect of the magnetic field alone, is under normal trapping conditions close to the true cyclotron frequency ω_c. The slower magnetron orbit, at frequency ω_-, is simply the result of the $\mathbf{E} \times \mathbf{B}$ drift. The condition $\omega_- < \omega_+$ is always true
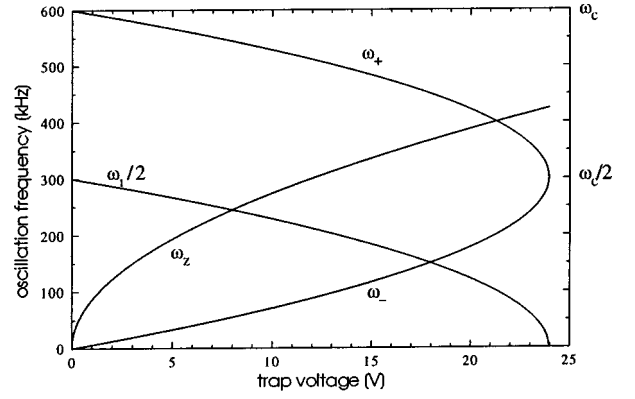

FIG. 2. Oscillation frequencies of a single particle in a Penning trap as a function of the trap voltage.

and with typical trapping parameters we have $\omega_- < \omega_z < \omega_+$. The oscillation frequencies as a function of the applied potential are plotted in Fig. 2. Unless specified otherwise, the values used throughout this paper are $B = 0.94$ T, $R_0^2 = 5.34 \times 10^{-5}$ m^2, $U_0 = 10$ V, and for magnesium ions the oscillation frequencies are then

$$\omega_z = 2\pi \times 276 \text{ kHz,}$$

$$\omega_- = 2\pi \times 72 \text{ kHz,}$$

$$\omega_+ = 2\pi \times 527 \text{ kHz,}$$

$$\omega_c = 2\pi \times 600 \text{ kHz,}$$

$$\omega_1 = 2\pi \times 455 \text{ kHz.}$$

The Hamiltonian for a single trapped particle can be written as [8]

$$H = \tfrac{1}{2}m\omega_1\omega_+ r_+^2 - \tfrac{1}{2}m\omega_1\omega_- r_-^2 + \tfrac{1}{2}m\omega_z^2 r_z^2. \tag{3}$$

We see that the energy associated with the magnetron motion is negative. That is, the magnetron motion is unbound and therefore ions confined in a Penning trap are in unstable equilibrium. This has the consequence that in order to cool the magnetron motion, that is, to reduce its kinetic energy or equivalently to reduce the amplitude of its motion r_-, energy must be added to this degree of freedom. This complicates seriously the application of laser cooling to the Penning trap.

B. Modeling of the atom-laser interaction

1. Laser beam

The laser beam is assumed to have a Gaussian profile. The diffraction of the beam is neglected, i.e., we keep the radius of the beam constant in its direction of propagation. This approximation is good as long as the spatial extension of the ions in the direction of the laser beam is smaller than the Rayleigh characteristic length of the Gaussian beam. For 280 nm radiation, a waist of 10 μm gives a Rayleigh length of 1.1 mm. Smaller beam waists are unlikely to be used as proper positioning of the waist would become difficult. This

approximation is equivalent to ignoring the component of the wave vector perpendicular to the beam.

The laser beam is assumed to be monochromatic. This is a good approximation as in most experiments the linewidth of the laser is much smaller than the natural linewidth of the cooling transition. We assume the laser beam remains in the radial plane parallel to the x axis. The laser intensity is given by

$$I(y) = \frac{2P_0}{\pi w^2} \exp\left\{-\frac{2(y-y_0)^2}{w^2}\right\}, \qquad (4)$$

where y_0 is the laser beam offset, w is the beam waist, and P_0 the total power. Unless specified otherwise, the values used throughout this paper are $w = 34\ \mu$m and $P_0 = 50\ \mu$W.

2. Scattering rates

The modeling of the interaction is based on the spontaneous scattering rate of the ion. It is assumed that the trapped ion can be properly approximated by a two-level system. The dynamics of the internal degrees of freedom of the ion is neglected. As a consequence, photon antibunching and quantum jumps, which, in magnesium or beryllium, can take place through a spontaneous Raman transition, are not taken into account. Photon antibunching can be neglected; since the time scale involved is much smaller than any motional frequency, it is not expected to have any influence on the ion dynamics in the regime of temperatures and oscillation frequencies studied in this work.

The semiclassical expression for the mean scattering rate of a two-level system in a laser field of frequency ω_l (wave vector $\mathbf{k}_l$) in the long-wavelength and rotating-wave approximations is given by [10]

$$\gamma_s = \frac{I\sigma_0}{\hbar\omega_l} \frac{(\Gamma/2)^2}{(\Gamma/2)^2 + \frac{I\sigma_0}{\hbar\omega_l}\frac{\Gamma}{2} + (\omega_0 - \omega_l + R/\hbar + \mathbf{k}_l\cdot\mathbf{v})^2}, \qquad (5)$$

where σ_0 is the scattering cross section at resonance, R is the recoil energy, and $\omega_0 - \omega_l$ is the detuning of the laser from resonance. With the laser beam parallel to the x axis we have $\mathbf{k}_l\cdot\mathbf{v} = k_l\dot{x}$. For magnesium as well as for beryllium we can safely ignore the recoil term compared to the other terms: $R_{Mg}/\hbar = 2\pi\times0.1$ MHz and $R_{Be}/\hbar = 2\pi\times0.2$ MHz. For magnesium, if we average over all polarizations of the incident laser we have $\sigma_0 = \lambda_0^2/2\pi$ with $\lambda = 280$ nm; for the $3p\ ^2P_{3/2}(M_J = -\frac{3}{2}) \to 3s\ ^2S_{1/2}(M_J = -\frac{1}{2})$ transition in ^{24}Mg$^+$ excited by light polarized perpendicular to the magnetic field, $\sigma_0 = 3\lambda_0^2/4\pi$. For Mg$^+$ the value of Γ is $2\pi\times43$ MHz. The average radiation force in the x direction exerted on the ion is then given by

$$F = F_x(y,\dot{x}) = \hbar k_l \gamma_s. \qquad (6)$$

C. Effect of a single scattering event on the motion of an ion

Consider a single trapped ion with magnetron radius r_- and cyclotron radius r_+. Its motion is given by the following equations (where we have dropped the initial phases φ_- and φ_+ without loss of generality):

$$x = x_- + x_+ = +r_-\cos\omega_- t + r_+\cos\omega_+ t, \qquad (7a)$$

$$y = y_- + y_+ = -r_-\sin\omega_- t - r_+\sin\omega_+ t, \qquad (7b)$$

$$\dot{x} = \dot{x}_- + \dot{x}_+ = -\omega_- r_-\sin\omega_- t - \omega_+ r_+\sin\omega_+ t, \qquad (7c)$$

$$\dot{y} = \dot{y}_- + \dot{y}_+ = -\omega_- r_-\cos\omega_- t - \omega_+ r_+\cos\omega_+ t. \qquad (7d)$$

On absorption of a photon k_l and spontaneous emission of a photon k_e the radii r_- and r_+ will be modified to r'_- and r'_+. Let $\Delta\mathbf{v} = (\mathbf{k}_l - \mathbf{k}_e)\hbar/m$ be the variation of the ion's velocity from the scattering of a photon ($\mathbf{k}_e$ is the wave vector of the emitted photon), then we have [6]

$$\Delta r_-^2 = r'^2_- - r_-^2 = \frac{\Delta v^2}{\omega_1^2} - \frac{2}{\omega_1\omega_-}\mathbf{v}_-\cdot\Delta\mathbf{v} \qquad (8a)$$

and

$$\Delta r_+^2 = r'^2_+ - r_+^2 = \frac{\Delta v^2}{\omega_1^2} + \frac{2}{\omega_1\omega_+}\mathbf{v}_+\cdot\Delta\mathbf{v}. \qquad (8b)$$

The $\Delta v^2/\omega_1^2$ terms represent the heating due to the discreteness of the interaction (recoil heating). Clearly, the magnetron radius will be reduced (cooled) when $\Delta\mathbf{v}$ is tangential to and in the same direction as the magnetron motion, while the cyclotron radius will decrease if $\Delta\mathbf{v}$ is tangential to and in the opposite direction to the cyclotron motion. This is a well known property (e.g., [6]). The cooling condition for the cyclotron motion is the same as for the cooling of the axial motion, while the condition for the cooling of the magnetron motion is just the opposite. This is of course simply a consequence of the respectively positive and negative contributions of the cyclotron and magnetron degrees of freedom to the total energy: energy must be extracted from the cyclotron motion, while it must be injected into the magnetron motion. It is well known that usually both degrees of freedom can be cooled simultaneously by detuning the laser *below* resonance and offsetting the beam on the side of the trap where the magnetron motion moves the ions away from the laser beam. In this way the ion will scatter more photons when the magnetron motion is moving it *away* from the laser rather than towards it (resulting in a cooling of the magnetron motion), and because of the higher cyclotron frequency, the ions will scatter more photons when the ions are moving towards the laser cooling beam (resulting in a cooling of the cyclotron motion). In fact as we will see below, this requirement is a consequence of the oscillation frequencies of the two motions: it is the difference between the magnetron and the cyclotron frequencies which allows laser cooling in the Penning trap, and as we will see, as these two frequencies get closer laser cooling becomes more difficult.

For our beam geometry, neglecting the small recoil term and averaging over all directions of the emitted photons, Eqs. (8) become

$$\Delta r_\pm^2 = \pm\frac{2}{\omega_1\omega_\pm}\dot{x}_\pm\Delta\dot{x}, \qquad (9)$$

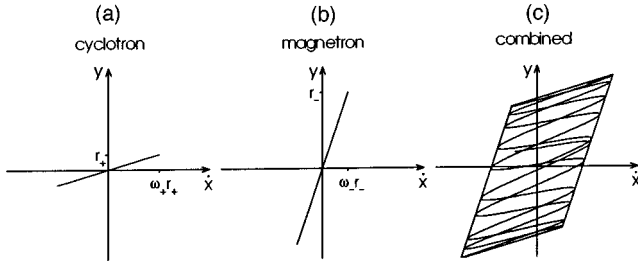where $\Delta\dot{x} = \hbar k_l/m$. In terms of the total energy we can write

FIG. 3. Orbit of a single trapped ion in the $\dot{x}$-y plane of phase space.

$$\Delta H_\pm = \pm \tfrac{1}{2} m \omega_1 \omega_\pm \Delta r_\pm^2 = m \dot{x}_\pm \Delta \dot{x}, \qquad (10)$$

$$\Delta H = \Delta H_+ + \Delta H_- = m(\dot{x}_+ + \dot{x}_-)\Delta \dot{x}. \qquad (11)$$

We see that in particular circumstances, scattering of a photon can result in no change in the total energy, but in a transfer of energy between the two degrees of freedom: the laser couples the two radial degrees of freedom.

Substituting for $\Delta \dot{x}$ and using Eq. (6), the average rate of change in these energies can be written as

$$\dot{H}_\pm = \dot{x}_\pm \hbar k_l \gamma_s(\dot{x}, y) \qquad (12)$$

and the total change in energy as

$$\dot{H} = \dot{H}_+ + \dot{H}_- = (\dot{x}_+ + \dot{x}_{-l})\hbar k_l \gamma_s(\dot{x}_+ + \dot{x}_-, y_+ + y_-). \qquad (13)$$

If we assume that the amplitude of one of the degrees of freedom is zero, the rate of change in the total energy simplifies to

$$\dot{H}_\pm = \dot{x}_\pm \hbar k_l \gamma_s(\dot{x}_\pm, y_\pm). \qquad (14)$$

This expression can also be written as a function of a single motional degree of freedom [Eq. (8)]

$$\dot{H}_\pm = \dot{H}_\pm(\dot{x}_\pm) = \dot{x}_\pm \hbar k_l \gamma_s(\dot{x}_\pm, \dot{x}_\pm/\omega_\pm) \qquad (15a)$$

or

$$\dot{H}_\pm = \dot{H}_\pm(y_\pm) = \omega_\pm y_\pm \hbar k_l \gamma_s(\omega_\pm y_\pm, y_\pm). \qquad (15b)$$

D. The phase-space picture

We have just seen that the scattering rate is a function of two variables, $\dot{x}$ and y; it is therefore natural to work in the plane of the phase space defined by these two variables. The motion of a single ion in that plane is simply

$$\dot{x} = \dot{x}_- + \dot{x}_+ = -\omega_- r_- \sin \omega_- t - \omega_+ r_+ \sin \omega_+ t, \quad (16a)$$

$$y = y_- + y_+ = -r_- \sin \omega_- t - r_+ \sin \omega_+ t. \qquad (16b)$$

The orbit of a pure magnetron/cyclotron motion will simply be a section of a straight line centered at the origin, of length proportional to the motion radius and with a slope of $1/\omega_\pm$. If both amplitudes are nonzero, the orbit will, in general, be an open curve which will fill a parallelogram as shown in Fig. 3. Only in the case when the ratio ω_+/ω_- is rational does the orbit become a closed curve. Clearly the cool-
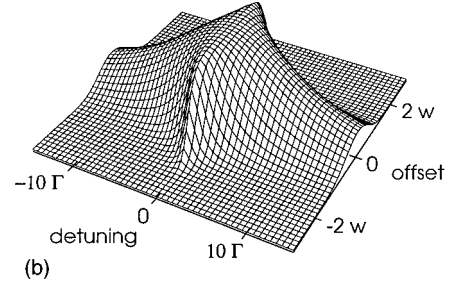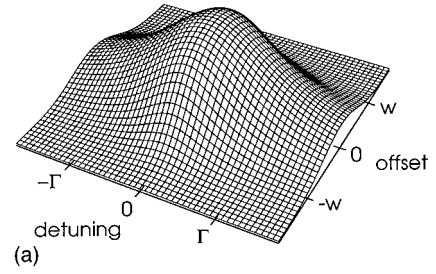

FIG. 4. Scattering rate as a function of laser detuning and offset. Laser power 50 μW (a) and 5 mW (b). The beam waist is 34 μm. Note the change of scale.

ing/heating of the ion's motion will strongly depend on the shape of $\gamma_s(\dot{x}, y)$; Fig. 4 shows plots of $\gamma_s(\dot{x}, y)$ as a function of the detuning $\Delta \omega = \omega_l - \omega_0$ and laser offset y_0 for low and high laser powers: clearly, very different results can be expected when saturation effects become important. This phase-space picture, by reducing the number of degrees of freedom, should make the study of laser cooling much more tractable. Besides its advantage of reducing the problem to only two variables, the scattering function has another very important and useful property: a change in the laser position along the y axis (the laser offset y_0) or a change in the laser detuning $\Delta \omega$ simply corresponds to an offset in our phase space $(\dot{x}, y)$ of $(-\Delta \omega/k, -y_0)$; identically these offsets can also be considered as a displacement of the origin of phase space in detuning-offset space.

E. Cooling condition

From Eq. (9) we have that the magnetron/cyclotron motion will be cooled/heated for that motion when $\dot{x} > 0$ and heated/cooled when $\dot{x} < 0$. Figure 5 illustrates this condition in phase space. Note that when the motion has both radii different from zero, the usual condition for the simultaneous cooling of both degrees of freedom, positive laser offset and negative laser detuning, is, to a first approximation, retrieved correctly.
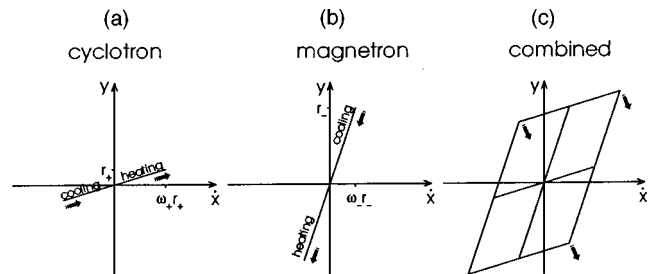

FIG. 5. Cooling condition for a single ion. The arrows indicate the effect of the laser on the amplitude of the motion.
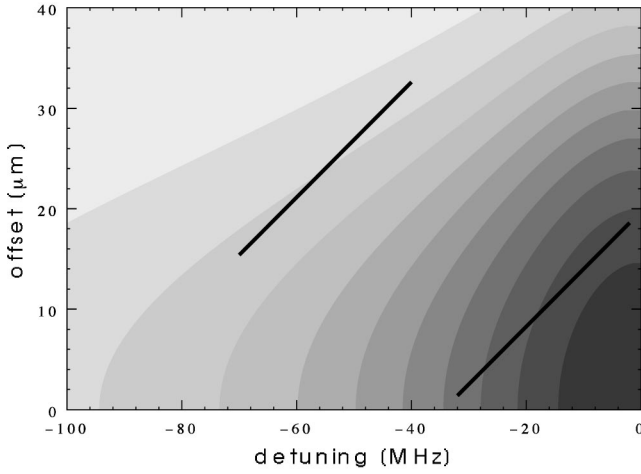
FIG. 6. Density plot of the scattering rate with two superimposed orbits of single ions in phase space with different laser offsets and laser detunings.

From Fig. 5 we see that the magnetron motion can be cooled thanks to the spatial inhomogeneity of the laser beam, while the cyclotron motion will be cooled because of the resonance line shape.

From now on, we assume that the motion of our ion is either pure cyclotron or pure magnetron (this condition will be relaxed in Sec. II H). We also assume for the moment that the amplitude of the motion is small enough that we can expand the scattering rate along the orbit in the form of a Taylor series. Keeping only the first two terms, we obtain

$$\gamma_s(\dot{x}, y) = \gamma_s(\omega_\pm y, y) = \gamma_{s\pm}(y) \cong \gamma_{0\pm} + \gamma_{1\pm} y. \quad (17)$$

This expression could of course be used to readily give a value for the ''temperature'' of the motion at equilibrium (see [6]). When $\gamma_{1\pm}$ is zero, the scattering rate is constant throughout the orbit and, if we neglect the recoil heating, the radius remains constant. If $\gamma_{1\pm}$ is different from zero, the motion will be either cooled or heated depending on its sign. The condition $\gamma_{1\pm} = 0$ defines, therefore, the heating/cooling boundary (neglecting the recoil heating). A clear physical picture is obtained by plotting the orbit on a contour plot of γ_s. As clearly visible from Fig. 6, the condition $\gamma_{1\pm} = 0$ is satisfied when the orbit is tangential to a contour line of γ_s. Therefore, if we calculate the slope, in detuning-offset space, of such a contour line we can readily find the boundary which delimits the cooling regions. The slope α of a contour line of fluorescence γ_0 is given by

$$\alpha = - \left. \frac{\partial \gamma_s}{\partial \Delta \omega} \right|_{\gamma_s = \gamma_0} \Bigg/ \left. \frac{\partial \gamma_s}{\partial y_0} \right|_{\gamma_s = \gamma_0}. \quad (18)$$

The slope of a pure motion in the laser offset-detuning phase space is $y/k_l \dot{x} = 1/k_l \omega_\pm$. The cooling boundary for the magnetron/cyclotron motion will be given by setting the slope of the curve of constant fluorescence equal to $1/k_l \omega_\pm$:

$$- \left. \frac{\partial \gamma_s}{\partial \Delta \omega} \right|_{\gamma_s = \gamma_0} \Bigg/ \left. \frac{\partial \gamma_s}{\partial y_0} \right|_{\gamma_s = \gamma_0} = 1/k_l \omega_\pm. \quad (19)$$
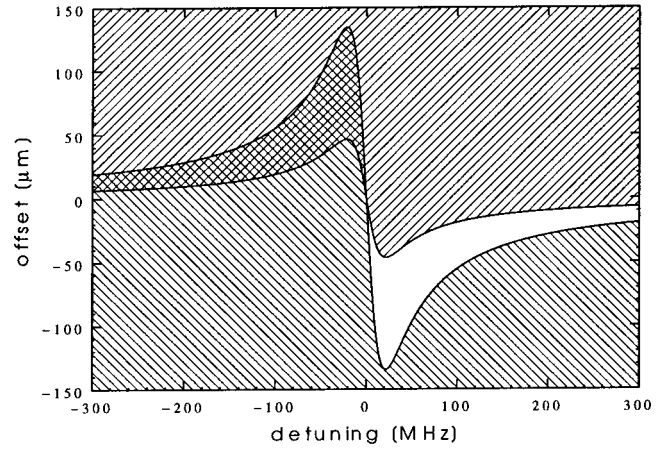
From the scattering rate defined by Eq. (5), we have

FIG. 7. Plot of the boundary function for the magnetron and cyclotron motions. The beam waist is 34 μm and the linewidth is $2\pi \times 43$ MHz. The positive hatching corresponds to regions where the magnetron motion is cooled, while the negative hatching corresponds to regions where the modified cyclotron motion is cooled. This plot is valid in the limit of small radii.

$$- \frac{\dfrac{I(y_0)}{dI(y_0)}}{dy_0} \frac{2\Delta \omega}{[(\Gamma/2)^2 + \Delta \omega^2]} = \frac{1}{k_l \omega_\pm}. \quad (20)$$

For a Gaussian beam as defined by Eq. (4), this becomes

$$- \frac{w^2 \Delta \omega}{2 y_0 [(\Gamma/2)^2 + \Delta \omega^2]} = \frac{1}{k_l \omega_\pm}. \quad (21)$$

Interestingly, this equation is intensity independent. As we will see later, this has important implications. This relation can be written in an explicit form:

$$y_0 = y_0(\Delta \omega) = -\omega_\pm \frac{\frac{1}{2} w^2 k_l \Delta \omega}{(\Gamma/2)^2 + \Delta \omega^2}. \quad (22)$$

This has the form of a dispersion curve. This function is independent of the laser power and scales in the y direction simply as the square of the beam waist. The curve has extrema of $\pm \omega_\pm w^2 k_l / 2\Gamma$ at $\mp \Gamma/2$, respectively. The two curves corresponding to ω_- and ω_+ are plotted in Fig. 7. The smallest curve corresponds to the magnetron motion: for laser offsets and detunings situated *above* this curve the magnetron motion is cooled (positive hatching), otherwise it is heated. For the cyclotron curve, which is larger because of the higher cyclotron frequency, the situation is inverted as the cooling/heating condition is the opposite of the magnetron condition. The cyclotron motion will therefore be cooled only when the laser detuning and offset are *below* the cyclotron curve (negative hatching). Therefore, the only region where both degrees of freedom are simultaneously cooled is the cross-hatched region. This result is valid in the limit of small radii, that is, usually at the latest stages of the cooling. This expression assumes a Gaussian beam profile, but the method used allows a similar condition to be calculated for any beam profile. Assuming a linear laser beam profile, we readily retrieve the cooling condition calculated by Itano and Wineland [6].

The consequences arising from these boundaries are numerous and have important implications, which we will discuss later. The simplicity of the cooling condition and its invariance on the laser power will make the discussion of laser cooling in the Penning trap much easier.

F. Numerical calculation

The analytical results obtained in the preceding section are only valid in the limit of small radii, so in order to consider larger radii we must use numerical methods.

If we consider just one degree of freedom, we can integrate the effect of the laser cooling over one period of that motion. For small amplitudes of the motion, the result should give us the same results as the analytical calculation done above. However, if we integrate for larger amplitudes we might find different results, in particular we might find some nontrivial steady states, that is, a steady state of one degree of freedom with a nonzero amplitude.

For a given amplitude of the motion we calculate the mean variation of its radius over one period of its motion:

$$
\begin{aligned}
\langle \Delta r_\pm^2 \rangle &= \pm \frac{\hbar k_l}{\omega_1 \omega_\pm} \frac{1}{T_\pm} \int_{-T_\pm/2}^{+T_\pm/2} \dot{x}_\pm(t) \gamma_s(\dot{x}_\pm(t), y_\pm(t)) dt \\
&= \pm \frac{\hbar k_l}{\omega_1} \frac{1}{T_\pm} \int_{-T_\pm/2}^{+T_\pm/2} r_\pm \sin \omega_\pm t \\
&\quad \times \gamma_s(r_\pm \omega_\pm \sin \omega_\pm t, r_\pm \sin \omega_\pm t) dt. \quad (23)
\end{aligned}
$$

This expression is of course valid as long as the effect of the laser cooling is small enough such that it does not significantly affect the scattering rate over one period. This expression does not take into account the effect of recoil heating. For a fixed laser detuning and offset, this expression gives us the mean heating/cooling rate of a pure magnetron or cyclotron motion as a function of the amplitude of that motion: $\langle \Delta r_\pm^2 \rangle = \langle \Delta r_\pm^2 \rangle (r_\pm)$. In particular, when the laser detuning and offset are within the boundaries defined by Eq. (22), we expect these quantities to be negative when $r_\pm$ tends towards zero. But a priori, this function can have any shape, and other zeros, at nonzero amplitudes, could be observed.

Figure 8(a) shows a plot of the heating rate for the cyclotron radius as a function of its radius, that is, $\langle \Delta r_+^2 \rangle (r_+)$. The laser detuning of -430 MHz and the offset of 20 μm lie outside of the cooling boundaries for the cyclotron motion, but within the cooling boundary for the magnetron motion. A positive value indicates heating, while a negative one indicates cooling. As expected, the motion is heated for small amplitudes, however for an amplitude of slightly more than 30 μm the curve crosses zero and for larger radii the motion is cooled. Therefore, if we assume that the magnetron motion is cooled and has a negligible amplitude, the cyclotron orbit will be "trapped" by the laser at a radius of about 30 μm. If its radius is less than this value, then it is heated, if it is larger, then it is cooled; this point is therefore a *stable* extremum.

Figure 8(b) shows another plot of the variation of the cyclotron radius as a function of its amplitude, but for a laser detuning of -10 MHz and an offset of 20 μm. In this case, the laser offset and detuning lie inside the stability region for both magnetron and cyclotron motions. Therefore for small
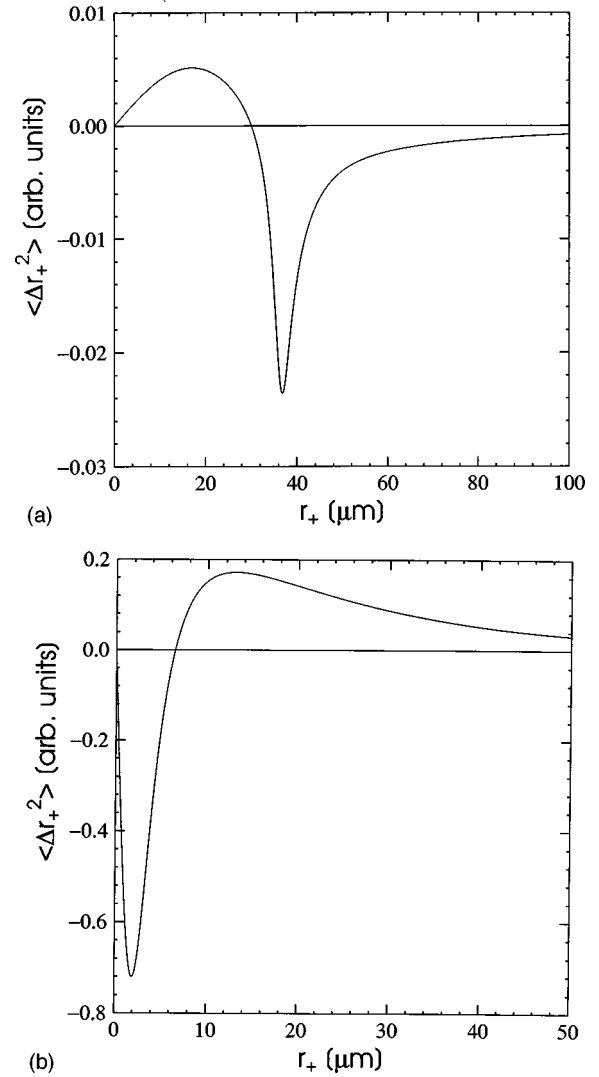

(a)

(b)

FIG. 8. Plot of the laser cooling/heating (in arbitrary units) of the cyclotron radius as a function of the radius. Positive values reflect heating, that is, an increase in the radius of the motion. The laser detuning and offset are -430 MHz and 20 μm (a) and -10 MHz and 20 μm (b).

radii, the cyclotron motion is cooled. However, for radii larger than about 6 μm, the motion is heated. This has the consequence that if initially an ion has a cyclotron amplitude of less than about 6 μm, it will be cooled further, but if larger than 6 μm, the ion will be heated.

It must be kept in mind that the results presented here for the cyclotron motion are only valid when the magnetron motion is neglected. The effect of nonpure motions will be discussed in Sec. II H.

G. Laser-trapped steady states

We are interested in studying the cooling rate as a function of the laser detuning *and* offset, so plotting $\langle \Delta r_\pm^2 \rangle (r_\pm)$ as a function of these quantities would result in four-dimensional plots. However, we are essentially interested in the presence of stable zeros. This information can simply be plotted in a two-dimensional detuning-offset plot using different symbols to indicate different conditions. The radius of the steady states can be plotted in the form of a
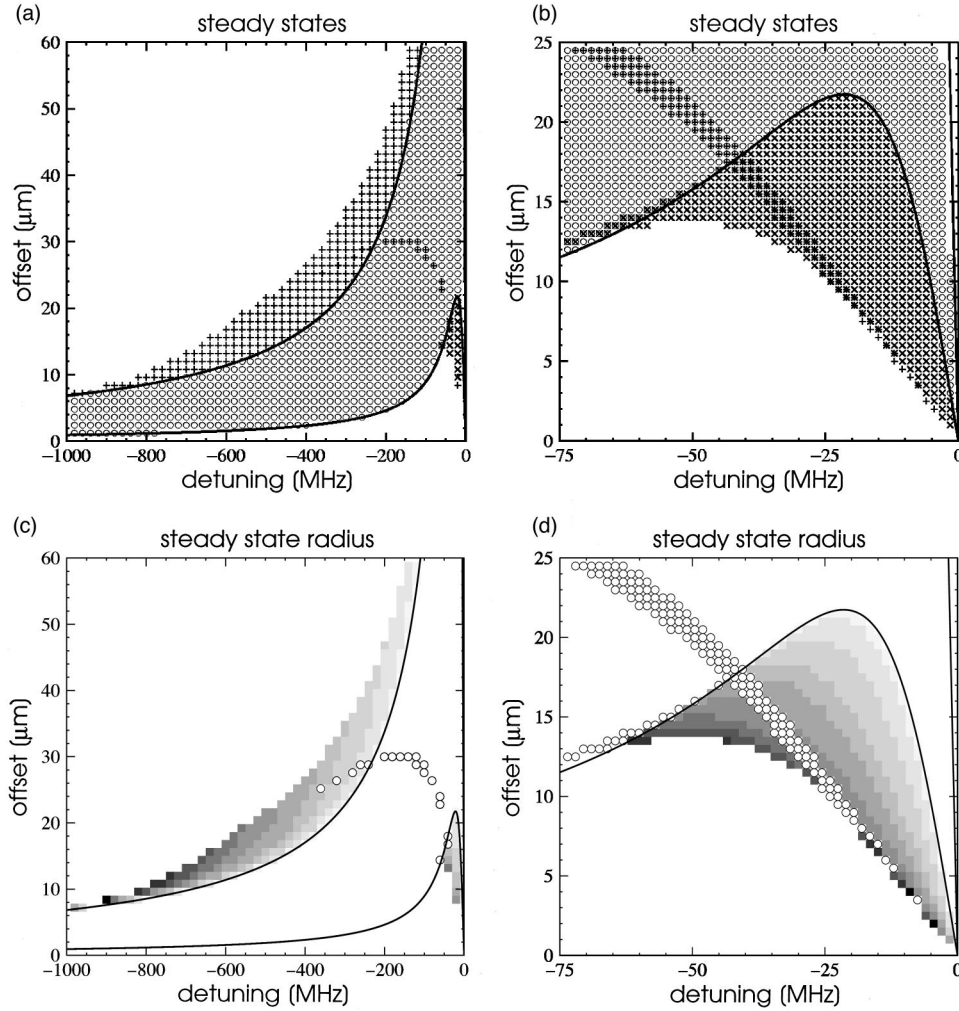
FIG. 9. (a,b) Cooling maps for a single ion. The various symbols represent the different laser cooled steady states: (○) both magnetron and cyclotron motions are cooled to zero radii, (×) nonzero radius steady states for the magnetron motion, and (+) for the modified cyclotron motion. The solid lines are the analytical cooling boundary functions. (c,d) Radius of the steady motion; darker grays indicate larger radii. The maximum radius is 54 μm in the magnetron region and 74 μm in the cyclotron region. The circles indicate the presence of steady states of large radii, but which seem to be relatively unstable.

density plot. We will call these plots ''maps.'' Figure 9 shows such maps for ^{24}Mg$^+$ with a beam waist of 34 μm and a laser power of 50 μW; the trapping potential is 10 V and the magnetic field is 0.94 T. In both maps, we have superimposed a plot of the boundary condition calculated from Eq. (22). As expected, the regions where both motions are cooled for small radii fit perfectly within the calculated boundaries. The regions where the steady-state cooled motion is not zero (laser trapped states) lie, as expected, outside, but very close to, these boundaries.

The line of open circles which crosses the stability region (more visible in the magnified plots) corresponds to the presence of additional zeros in the cooling rate at larger radii. Their position is very sensitive to the laser detuning, offset, power, and waist size. In addition, the cooling rate at these zeros is very weak. Therefore, we do not expect them to be of much experimental significance.

Also in Fig. 9 is a density plot of the radius of the laser-trapped steady states. As can be seen by looking at Fig. 10, these laser-trapped steady-state regions are remarkably independent of the laser power and scale very much like the

square of the laser waist size. This means that these regions seem to obey the same scaling rules as the cooling boundaries.

We see that at high trap voltages (21 V is the voltage at which the modified cyclotron frequency is equal to the axial frequency) the cooling region shrinks to a very small area. At very small voltages, the laser-trapped steady-state region vanishes, while it increases for high voltages.

H. General motion

Until now we have assumed that the motion of the single particle was either purely magnetron or cyclotron. This assumption allowed us to integrate the effect of the laser beam over one period of the motion as a function of the motion radii. The result of the integration was conveniently plotted in the form of maps. This was possible because we were only interested in the presence of zeros or in the slope of the heating/cooling curve [Eq. (23)]. Now, by allowing for both magnetron and cyclotron radii to be simultaneously different from zero, we add one degree of freedom in the integration
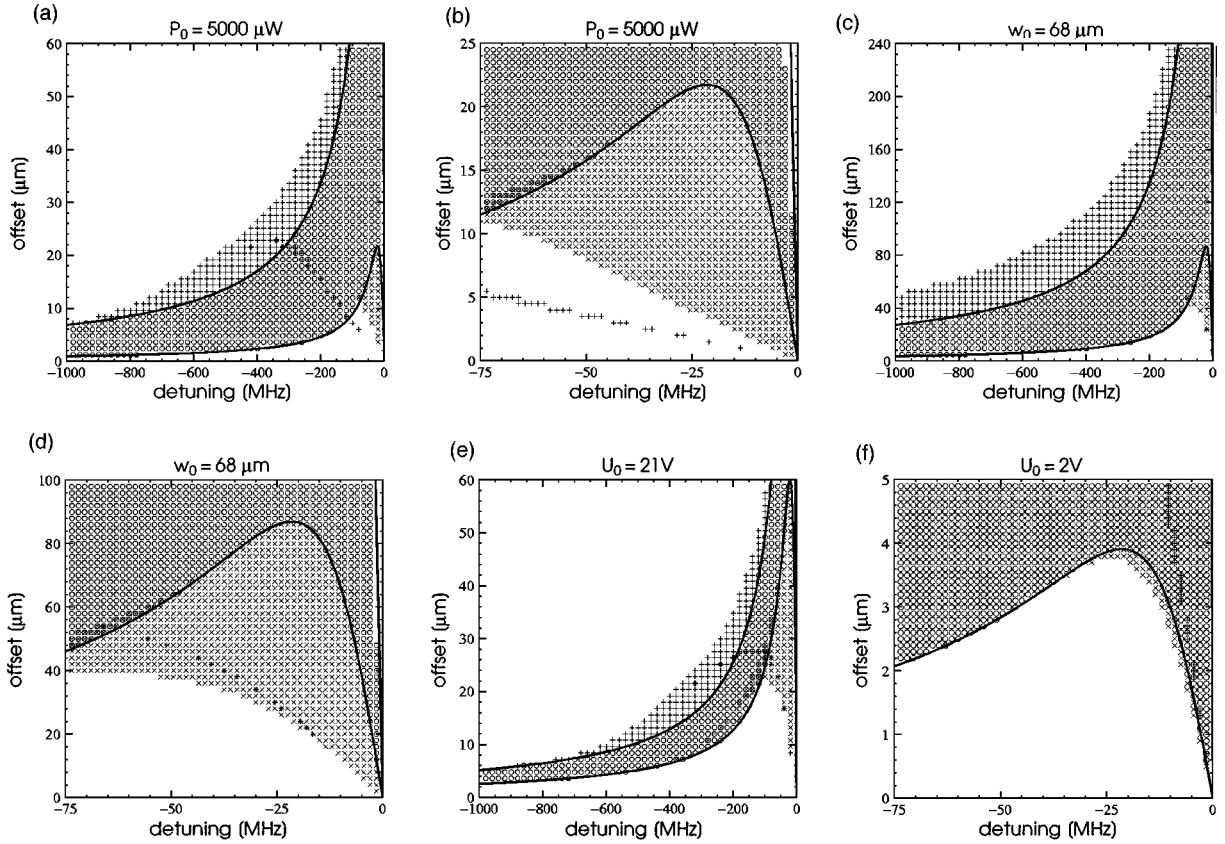
FIG. 10. Same as Fig. 9, but for larger laser power (a,b) and larger beam waist (c,d) and different trap voltages (e,f).

calculation and the resulting function has two degrees of freedom. The result of this integration can be conveniently plotted in the form of a two-dimensional vector field as shown in Fig. 11. On this plot, an arrow pointing towards the left/right indicates a cooling/heating of the magnetron motion, while an arrow pointing down/up indicates a cooling/heating of the cyclotron motion. In this way, the arrow indicates the direction of the variation of the ion radial orbit. Along the plot axes, $r_+ = 0$ or $r_- = 0$, we retrieve the pure motion results. Similarly to what we have done for the pure motion case, we could, in principle, extract from these vector fields all relevant topological features and plot the result in a detuning-offset map. However, a proper topological analysis of these vector fields is in fact a very difficult task. Moreover, the calculation of such a map would require too much processing time to be practical. As a consequence, we will simply determine whether, for *fixed* magnetron and cyclotron radii, the magnetron and cyclotron degrees of freedom are cooled or heated as a function of laser offset and detuning. The result can again be plotted in the form of a map, the points where the magnetron and cyclotron degrees of freedom are cooled being indicated by different symbols (see Fig. 12). In the case where r_+ and r_- are both small, we retrieve the earlier results [Fig. 12(a)]. As a single ion is loaded, the energy distribution between its three degrees of freedom is unknown. The initial state of the ion can therefore take any form. In order to simplify the problem, we will limit our calculations to three particular cases: $r_+ \ll r_-$, $r_- \ll r_+$, and $r_- \approx r_+$. However, it can be easily shown that

assuming a random distribution in velocity and position, the magnetron radius r_- will, in general, be larger than the cyclotron radius r_+.

1. The $r_- \gg r_+$ case

In the normal case, we essentially observe a dramatic extension of the cooling region towards negative detunings [Figs. 12(b) and 12(c)]. There is no significant extension
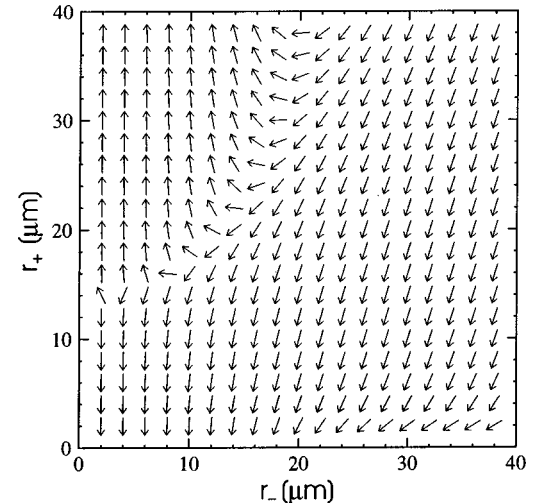

FIG. 11. Vector field of the variation of the magnetron and cyclotron radii under the effect of the laser.
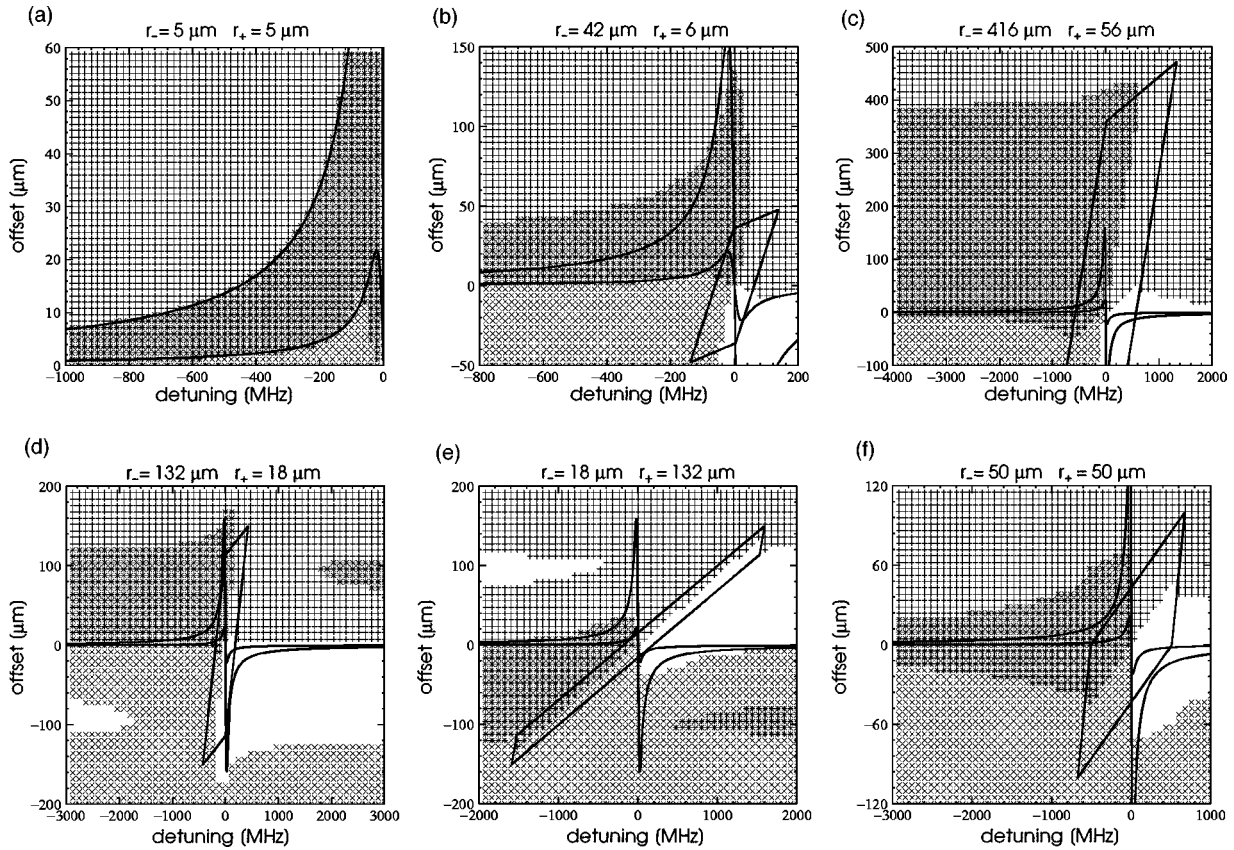
FIG. 12. Maps of the cooling for nonpure radial motions. ×, cooling of the cyclotron motion; +, cooling of the magnetron motion. Note the symmetry of the various regions.

towards larger laser offsets; this is due to the fact that the parallelogram where the cyclotron motion is heated extends further up, in offset, than the parallelogram where the cyclotron motion is cooled. Although the same is true of the magnetron motion, the fact that a Gaussian (beam profile) dies off much more quickly than a Lorentzian (resonance line shape) prevents a similar result. This band keeps its width, equal to approximately the magnetron radius, to infinite negative detunings. In addition to this region, we still have the pure motion cooling regions and of course also the top left parallelogram of the ion orbit [see Fig. 5(c)].

Interestingly, a new, completely unexpected, cooling region appears for laser detunings *above* resonance [Fig. 12(d)]. The cooling of the magnetron motion in this region is expected as the offset is positive, but the cooling of the cyclotron motion is surprising. We normally expect the cyclotron motion to be cooled only for negative laser detunings, because we want to have more scattering in the ''cooling'' half of the parallelogram than in the ''heating'' half. However, the fact that the cyclotron motion is not parallel to the laser beam, and is ''carried'' through the beam by the magnetron motion, allows for a subtle effect. When the center of the cyclotron motion reaches the laser beam from positive values of the laser offset, only the cooled side of the cyclotron motion is in the laser beam, therefore the motion is cooled (see Fig. 13). When the cyclotron motion is on the other side of the beam, only the heated side is in the beam and the motion is heated. If the laser is detuned above resonance, there is more scattering on the heated side than on the

cooled one, and we expect the motion to be, overall, heated. But, in fact, because the magnetron is ''taking'' the cyclotron motion from one side of the beam to the other, the ion is spending more time on the side where the motion is cooled than on the side where the motion is heated. If the time difference is large enough (due to beam position and width), the difference between heating and cooling due to the laser offset can be compensated by the time difference. All the motions have a $\sin \omega t$ dependence, and therefore the largest time difference takes place near the motion extremum. As is
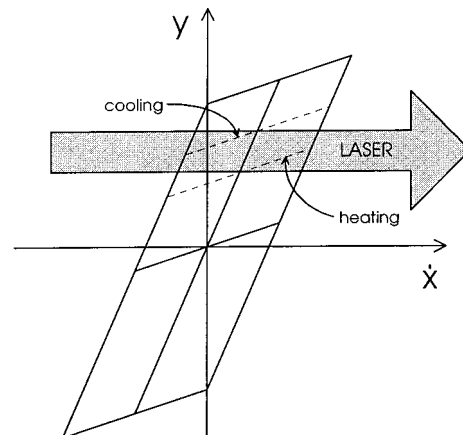

FIG. 13. Diagram illustrating the overall cooling of the modified cyclotron motion as it is ''displaced'' by the magnetron motion. The dotted line approximates the cyclotron motion.
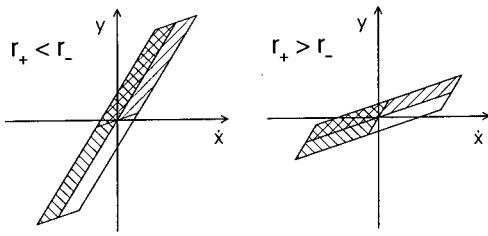
FIG. 14. Illustration of the displacement of the cooling parallelogram halves when the cyclotron radius is much smaller or larger than the magnetron radius. The shaded areas indicate cooling.

clearly visible in Fig. 13, this corresponds very well to the position of the cooling band. The time difference can only compensate for small scattering differences, that is, small slopes in the resonance line shape. We therefore expect the position of the band to move closer to resonance for larger linewidth, especially for higher laser powers.

2. The $r_- \ll r_+$ case

In this case, the result is similar to the previous one, with the difference that both cooling bands are now for negative offsets [Fig. 12(e)]. This may seem surprising, but in fact is simply due to the large cyclotron motion which takes the cooling parallelogram to mainly negative offsets (see Fig. 14).

3. The $r_- \approx r_+$ case

For small detunings, we essentially have the combined effect of large magnetron and cyclotron radii. However, for larger detunings, the width of these cooling bands rapidly decreases [see Fig. 12(f)].

Overall, we essentially have that for nonpure motions, the cooling regions are extended towards very large negative detunings. The presence of bands for positive detunings is unlikely to be of much practical importance, but is a good illustration of the actual complexity of perpendicular laser cooling in the Penning trap. When the radii involved are small such that the ion's orbit in phase space is much less than the beam waist and the resonance linewidth, we retrieve the results obtained analytically [see Fig. 12(a)].

I. Tilted beam

If the beam is not parallel to the radial plane, the x coordinate of the ion's motion must be taken into account and we lose the advantage of being able to simply superimpose the ion orbit and the laser scattering rate in a two-dimensional plot. However, most results obtained in this section are qualitatively valid. And for relatively small angles of tilt (approximately 10°–20°), the maps obtained numerically remain, to a very good approximation, valid. It is only for larger angles that significant quantitative changes are visible. When both magnetron and cyclotron radii are nonzero, the effect of a tilted beam seems to be much more dramatic (see Fig. 15). The cooling band at positive detunings is strongly widened and is connected to the negative detuning cooling regions. In this plot, the shape of the cooling limits takes again the shape of a dispersion curve. This means that it might be possible to calculate all cooling regions using appropriately offset dispersion curves.
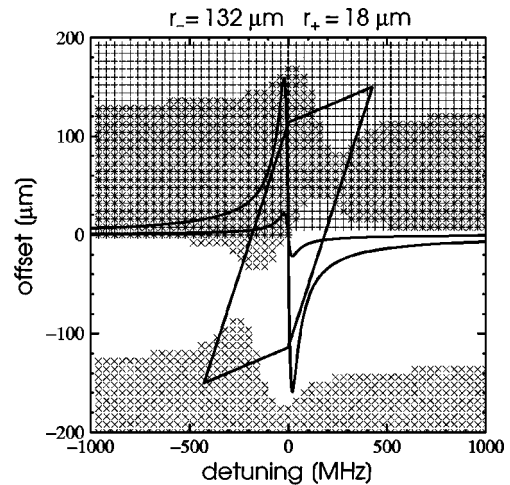

FIG. 15. Map for the case of a laser beam oriented at 45° in the x-z plane, and going through the y axis.

J. Discussion

1. Axial motion

In this section we have completely neglected the axial degree of freedom. In fact, as we saw in most cases, a change in the laser power does not significantly change the cooling dynamics. Although the beam waist strongly affects the cooling regions, this is of no importance with Gaussian beams, as their widths are independent of the position. Therefore, to a first approximation, the presence of axial motion should also not change the results obtained here. However, it is important that the axial motion be cooled, as otherwise it would be heated by the recoil heating. Cooling of the axial motion can be achieved by either using a second beam oriented along the z axis or by tilting the perpendicular cooling beam. If the angle of tilt is small, the main features described in this section remain valid, while the axial motion will be cooled (so long as the detuning is negative.)

2. Temperature of a single ion

Clearly, the phase-space picture developed in this section is very well suited to calculate the temperature of a single ion in the steady state. The principle of the calculation would be similar to the calculation carried out by Wineland and Itano [6].

3. Effect of the recoil heating

In some cases, the cooling rate from the laser beam might be smaller than the recoil heating rate. In such cases, the motion would not remain confined. However, we expect these effects to be limited to very small parts, close to the boundaries of the cooling regions.

4. Comparison with experimental observations

The existence of ''laser-trapped'' steady states was proposed and numerically verified by Wilson as an attempt to explain the presence of a modulation of the fluorescence from single ions [5]. This, sometimes strong, modulation at twice the magnetron frequency was in fact observed in the photon-photon time interval distribution [11]. This explana-

tion was necessary because a single ion at its minimum temperature would not have a large enough radius to modulate the scattered light by Doppler shift and/or by spatially moving across the laser beam. (Although this modulation might be due to the presence of impurity ions.) Here we have confirmed the existence of these ''laser-trapped'' steady states and demonstrated their stability. The position of the region of these states in detuning-offset space explains very well why a modulation was so often observed in Wilson's work. Experimentally, once an ion was loaded, the laser offset was kept constant and the laser was tuned from several gigahertz below resonance towards resonance. If we look at Fig. 9, it is clear that by following this experimental method, we are very likely to reach these ''laser-trapped'' steady states.

Modulation of the fluorescence of a single ion at the modified cyclotron frequency has not been observed. This is probably due to the fact that these regions are situated at relatively large detunings, where the fluorescence level can be close to the background scattering rate. The presence of a single ion was inferred from the observation of quantum jumps, which, in magnesium, can only be observed for large scattering rates. Therefore, it was normal to try to maximize the scattered fluorescence by tuning the laser as close as possible to resonance, which means that the actual observation of a modulation at twice the modified cyclotron frequency was very unlikely.

The results obtained so far for the laser cooling of a single ion explain the relative difficulty in laser cooling a single ion, in particular the extreme sensitivity on the laser offset.

5. Recipe for the laser cooling of a single ion

We can now propose some general rules which should help in the laser cooling of a single ion. The goal is to find the optimum trapping parameters for the cooling of a single ion. For a given set of trap parameters, we also want to find the optimum laser detuning and offset, such that all degrees of freedom are simultaneously cooled independently of their amplitudes. The variable parameters are the two radial oscillation frequencies (which depend on the electric potential, magnetic field, trap dimensions, and the ion mass and charge), laser waist size, ion resonance linewidth, and finally laser power. Note that some of these laser cooling requirements may conflict with desirable trapping parameters so that in some cases a compromise is necessary (e.g., in the choice of ion mass).

Trap voltage. The trap potential should be low. In this way the cooling region is larger and when approaching resonance from large detunings it is possible to get closer to resonance without having to change the beam offset. Field imperfections such as a contact potential can of course put a limit on the lowest practically achievable potential [11].

Magnetic field. A strong magnetic field is required. The larger the magnetic field, the larger the cyclotron frequency will be and the greater the cooling region will be.

Laser beam waist and power. In order to achieve high cooling rates, it seems preferable to have a large beam waist rather than a high laser power. More importantly, a large beam waist would allow for a less accurate and less stable beam positioning system.

Ion species. The trapped species should be light; this would lead to a large cyclotron frequency and therefore to

larger cooling regions. A strong cooling transition would allow faster cooling but higher minimum velocities.

Beam offset and laser detuning. Ideally, in order to achieve fast cooling of a single ion, the laser beam offset and detuning should ''follow'' the maximum spatial extent of the ion orbit. However, this is usually impossible as the actual orbit is unknown. It is therefore probably safer to set the laser detuning and offset to fixed values at which the motion is cooled whatever its orbit. In practice, this means a laser detuning of a few linewidths below resonance and a beam offset of one beam waist, the exact values depending of course on the actual setup.

III. LASER COOLING OF THE TWO-ION CRYSTAL

A general study of the laser cooling of two trapped ions in a Penning trap is a very complex problem, as in general, the motion of two ions is chaotic. However, the laser cooling force can be very strong and can quickly cool two ions to a crystalline state [12], whose motion has been extensively studied [5,13–15]. We will therefore concentrate on the study of steady states of the two-ion crystal in the presence of laser cooling.

The laser cooling of two ions in the Penning trap is a very different problem from the cooling of a single ion. First we have, in the radial plane only, four degrees of freedom. Second, the dynamics of the motion is strongly nonlinear. The first consequence is that we will not look here for expressions of the form of Eq. (9) for the effect of a single scattering event on the four degrees of freedom of our two-ion system. The second consequence is that although the motion can be decoupled into center of mass and relative motions, the presence of the laser cooling will actually couple them. This coupling will, in general, be very weak. Finally, when in a radial crystal state, the rotation frequency of the ions depends on their separation. This is completely different from the case of a single ion and, in particular, the radius of the motion, for a radial crystal, is never zero [14].

We will in general neglect the center-of-mass motion. Wilson showed in the case of two ions that the center-of-mass motion was, as expected, strongly laser cooled [5]. In fact, as long as the separation between the two ions is large enough, the motion of each ion will be nearly identical to the motion of a single ion and if the laser parameters are such that the motion of a single ion is cooled, both ions will be cooled and therefore the center-of-mass motion will also be cooled. In the presence of strong laser cooling, which is necessary for obtaining a crystal configuration, the amplitude of the center-of-mass motion is in general much smaller than the amplitude of the relative motion. We will therefore, in general, ignore the center-of-mass motion.

A. Motion of two-ion crystals

We define a crystal as a configuration where the distance between the two ions is roughly constant. The crystal will have three possible orientations: it will be aligned either along the z axis or in the radial plane or tilted at an angle between these two configurations. Here we concentrate on the laser cooling of a radial crystal and therefore restrict our calculations to the radial plane. For large ion separations, the radial configuration is always possible, however for smaller
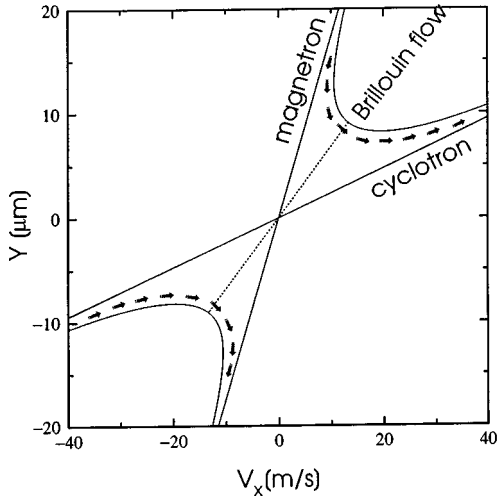
FIG. 16. Orbit of a two-ion crystal in phase space as the crystal goes from a large radius in magnetron mode to a large radius in cyclotron mode. The arrows indicate the effect of the interaction with the laser cooling beam on the crystal radius.

separations the crystal can be tilted or aligned along the z axis. In the case of a tilted configuration, the crystal rotation frequency is constant, i.e., it does not depend on the crystal angle of tilt. In the axial configuration, the ions are essentially at rest; their magnetron and modified cyclotron oscillation frequencies are slightly modified by the Coulomb interaction.

The relative motion of a two-ion crystal is characterized by two parameters, the distance between the ions ($2r_0$) and the crystal angular velocity (ω_r). These two quantities are related through the following equations [5,14]:

$$\omega_{r,\pm}(r_0) = \frac{1}{2}\left[\omega_c \pm \left(\omega_1^2 - \frac{Q}{r_0^3}\right)^{1/2}\right], \tag{24}$$

where $Q = q^2/4\pi\varepsilon_0 m$ and q is the electrical charge of one ion. In the limit of large separation, the rotation frequency tends towards ω_+ or ω_-. The minimum separation is reached as expected when the crystal rotates at half the true cyclotron frequency ($\omega_r = \frac{1}{2}\omega_c$), and is

$$r_{0,\text{min}}^3 = \frac{Q}{\omega_1^2}. \tag{25}$$

At minimum separation, maximum ''density,'' the crystal is said to be at Brillouin flow.

B. Motion of two ions in phase space and the cooling condition

In phase space, the orbit of the relative motion of a two-ion crystal will, as for a single ion, be a section of a straight line, but the slope of that line will depend nonlinearly on the amplitude of the motion. For large separations, the crystal will rotate at the magnetron or modified cyclotron frequencies; as the ions' separation decreases, their rotation frequency increases from the magnetron frequency or decreases from the modified cyclotron frequency. At minimum separation (Brillouin flow) the crystal rotates at half the true cyclotron frequency. Figure 16 shows a plot of the envelope of the

orbit of the relative motion of a two-ion crystal in phase space as its rotation frequency varies from ω_- to ω_+. The cooling condition for the two-ion crystal can be deduced by comparing with the cooling of a single ion. As long as the crystal is in the magnetron mode, energy must be added to this degree of freedom in order to reduce its amplitude. When the crystal is in the cyclotron mode, energy must be removed from this degree of freedom in order to reduce its amplitude. At Brillouin flow, the radius is at its minimum value and can therefore *not* be reduced any further. As for a single ion, the motion is circular and therefore when the crystal is in the magnetron mode, its radius will be reduced for $\dot{x} > 0$ and increased when $\dot{x} < 0$ [Eq. (9)]. For a crystal in the cyclotron mode, the opposite will be true. Figure 16 summarizes the heating/cooling condition. At Brillouin flow, if $\dot{x} < 0$, the radius increases and ω_r decreases (in absolute value), and the crystal goes into the magnetron mode, while if $\dot{x} > 0$, the radius and ω_r increase, and it goes into the cyclotron mode.

Looking at Fig. 6, we clearly see that a steady state will be attained when the ion's orbit is parallel to the lines of constant fluorescence. While for a single ion the slope of the orbit is constant, the slope of the orbit of a two-ion crystal can vary between $1/\omega_-$ and $1/\omega_+$. Let us assume that the slope of the curve of constant fluorescence is between $1/\omega_-$ and $1/\omega_+$, that is, the laser detuning and offset lie within the laser cooling boundary for a single ion. If the ion crystal has a large radius in the magnetron mode as illustrated in Fig. 16, the scattering rate is stronger on the $\dot{x} > 0$ side. This will be the case until the slope of the orbit is parallel to the slope of the curve of constant fluorescence. Similarly, if we start with a large crystal in the cyclotron mode, the scattering rate will be stronger on the $\dot{x} < 0$ side of the orbit, the radius will therefore decrease until it reaches the Brillouin flow, and at that point the radius will increase but the angular frequency will keep decreasing and the crystal goes into the magnetron mode; at that point the radius increases until the slope of the orbit is parallel to the curve of constant fluorescence.

What happens is that the interaction of the crystal with the laser cooling field aligns the orbit of the crystal parallel to the fluorescence contour lines. Or equivalently, the crystal rotation frequency ''locks'' to the fluorescence contour lines.

If the orbit of the crystal is small enough, we can obtain from Eq. (22) the rotation frequency of our crystal in its steady state as a function of the laser detuning and offset:

$$-\omega_r(\Delta\omega, y_0) = \frac{2y_0}{k_l w^2 \Delta\omega}[(\Gamma/2)^2 + \Delta\omega^2]. \tag{26}$$

Using Eq. (24), we can express the radius of the two-ion crystal as a function of the laser detuning and offset:

$$r_0^3(\Delta\omega, y_0) = \frac{Q}{4\{\omega_1^2 - [\omega_r(\Delta\omega, y_0) + \omega_c/2]^2\}}. \tag{27}$$

In particular, Eq. (22) gives us the line, in detuning-offset space, along which the crystal is at Brillouin flow:

$$y = y(\Delta\omega) = -\frac{\omega_c}{4}\frac{w^2 k_l \Delta\omega}{(\Gamma/2)^2 + \Delta\omega^2}. \tag{28}$$

These expressions are only approximations where we have assumed, in detuning-offset space, the crystal orbit to be much smaller than the extension of the fluorescence function γ_s. We will now compare these analytical expressions with numerical calculations which will fully take into account the topology of γ_s.

C. Numerical calculations

As before, for simplicity we will assume that the center-of-mass motion has zero amplitude. We will also ignore the small oscillation of the crystal about its steady motion. This means that as in the single ion case, we will consider only one degree of freedom. We will also neglect the recoil heating. Let us find an expression for the variation of the radius of the crystal due to a single scattering event. We saw for the single ion case that the change in the square of the radius of the motion was simply proportional to the scalar product of the ion velocity and the velocity change $\Delta\mathbf{v}$. We assume that the same is true for the case of a two-ion crystal:

$$\Delta r_0^2 \propto \pm\, \mathbf{v}\cdot\Delta\mathbf{v}, \qquad (29)$$

the sign being positive for a crystal in the cyclotron mode and negative for a magnetron crystal. As for a single ion, we will integrate the effect of the laser scattering over one period of the motion; again we assume that the motion is not perturbed significantly by the laser during the integration period. For a given radius of the motion, we calculate the variation of its radius over one period of its motion:

$$\langle\Delta r^2(r)\rangle_{T(r)} \propto \pm\langle\Delta H(r)\rangle_{T(r)}$$

$$\propto \pm\frac{1}{T(r)}\int_{-T(r)/2}^{T(r)/2} r\sin\omega_r(r)t\,\gamma_s(\dot{x}(t),y(t))dt$$

$$\propto \pm\frac{1}{T(r)}\int_{-T(r)/2}^{T(r)/2} r\sin\omega_r(r)t$$

$$\times\,\gamma_s(r\omega_r(r)\sin\omega_r(r)t, r\sin\omega_r(r)t)dt \qquad (30a)$$

or equivalently

$$\langle\Delta r^2(\omega_r)\rangle_{T(r)} \propto \pm\frac{1}{T(r)}\int_{-T(r)/2}^{T(r)/2} r(\omega_r)\sin\omega_r t$$

$$\times\,\gamma_s(r(\omega_r)\omega_r\sin\omega_r t, r\sin\omega_r t)dt. \qquad (30b)$$

As for the single ion case, this expression will only be valid as long as the effect of the laser cooling on the actual motion is small enough not to significantly affect the scattering rate in one integration period. Figure 17 shows an example of the heating/cooling of the radius of the two-ion crystal as a function of its rotation frequency. In this case the laser detuning and offset lie within the single ion cooling boundaries. This means that for large ion separations the motion is cooled. For a large magnetron mode crystal, energy is added to the crystal (negative slope), and for a large cyclotron mode crystal, energy is removed from the crystal (positive slope). Therefore, by continuity, there must be a crystal radius (or rotation frequency) at which there is no net change in the crystal energy. This happens here at slightly below half the true cyclotron frequency (Brillouin flow). At
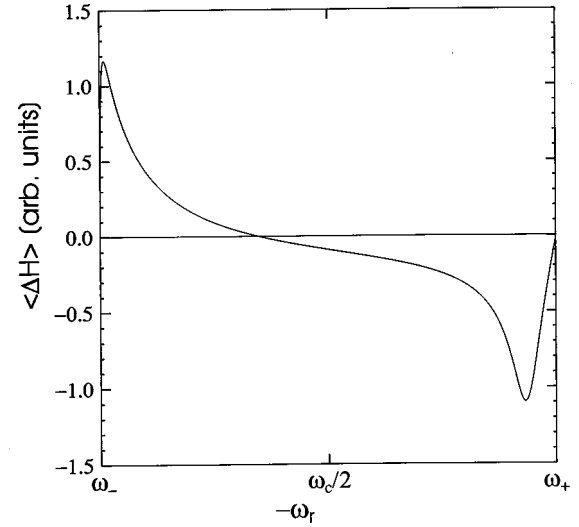

FIG. 17. Plot of the mean variation of the radius (in arbitrary units) of a two-ion crystal as a function of the crystal rotation frequency.

this point, the cooling and heating effect from the laser cooling beam exactly balance each other. As we want to study the steady state of the laser cooled crystal, we are only interested in the position of the zero. As in the case of the single ion, we can plot the relevant features (magnetron/cyclotron mode, crystal radius, etc.) in the form of maps.

D. Maps

Figure 18 shows the regions where a two-ion crystal is stable in the laser detuning-offset space. Also plotted is a density plot of the radius of that stable crystal. Despite the relatively large ion separation (around 18 μm at Brillouin flow in this case), the stability regions of the two-ion crystal are very similar to the single ion case (where the calculation was done in the limit of zero radii). At the single ion cooling boundaries (indicated by two solid lines on the plots), the ion separation is the largest, and its rotation frequency tends towards the single ion magnetron or modified cyclotron frequencies. The middle solid line indicates where the slope of constant fluorescence corresponds to the slope of a motion at half the true cyclotron frequency, i.e., at Brillouin flow. We see that this Brillouin line fits very well with the boundary between the $+$ and $\times$ crosses, which corresponds to the regions where the crystal is in the cyclotron and magnetron mode, respectively.

As can be expected, the regions where a single ion is in a laser-trapped state correspond to the largest crystal separations. From these similarities, it is expected that these maps will obey the same scaling rules as the single ion ones for varying laser power and beam waists (see Fig. 18). It has been verified that the steady-state regions remain well defined by the single-ion cooling boundaries in the limit of zero laser beam waists.

E. Comparison with numerical simulations

In Fig. 19 we have plotted the radius of the crystal as a function of the detuning for a fixed offset. For comparison
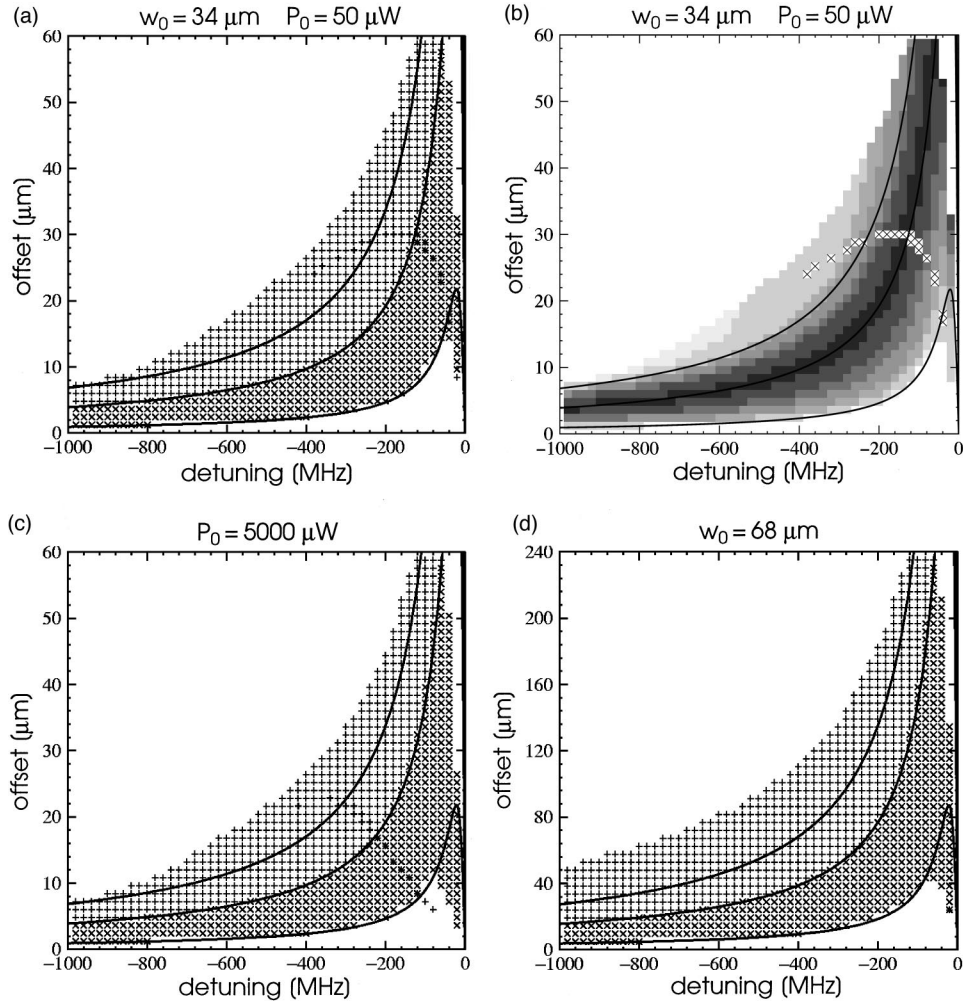
FIG. 18. Maps for two-ion crystals: $\times$, the crystal is in the magnetron mode; $+$, cyclotron mode. The solid lines indicate the single-ion cooling boundaries and the Brillouin flow condition. (a) The beam waist is 34 μm and the laser power is 50 μW. (b) Density plot of the crystal separation. Darker grays indicate smaller distances. (c) Same as top left but with a laser power of 5 mW. (d) Same but with a laser beam waist of 68 μm.

we have also plotted the value of the radius calculated from Eq. (27) and the radius obtained from numerical simulations. These numerical models are described elsewhere [16]. Two types of numerical models were implemented: in the ''radiation pressure'' model, the interaction with the laser beam is considered in the semiclassical limit, that is, the light force is assumed to be continuous, that is, the discreteness of the interaction is neglected. In the ''recoil'' model the interaction with the laser beam is modeled at the photon level: the mechanical effect of each fluorescence photon is taken into account.

In the recoil model the radii are obtained by averaging over 200 ms of simulation; the error bars correspond to the standard deviation obtained by averaging ten periods of 20 ms. We see that even when the recoil heating is taken into account, the cooling rate is high enough to damp the crystal's small oscillations. The agreement between the three numerical calculations is remarkable. In particular, the analytical calculation of the crystal radius as a function of the laser offset and detuning [Eq. (27)] is in very good agreement with the full numerical treatment within the single ion cooling boundaries. This shows that the simple calculation of the
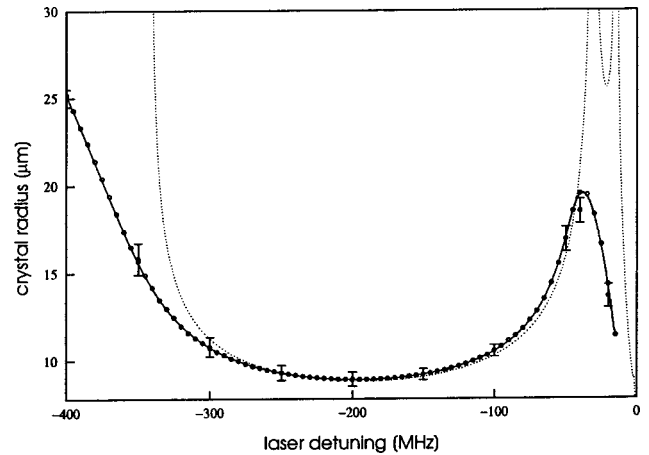

FIG. 19. Plot of the radius of a two-ion crystal as a function of the laser detuning for an offset of 20 μm. The circles correspond to the zeros of Eq. (30), the solid line is obtained from the simulation in radiation pressure mode by scanning the laser detuning ''adiabatically.'' The dotted line is the radius calculated using Eq. (27). The solid circles are from the simulation using the recoil model, the error bars correspond to the standard deviation of the radius.
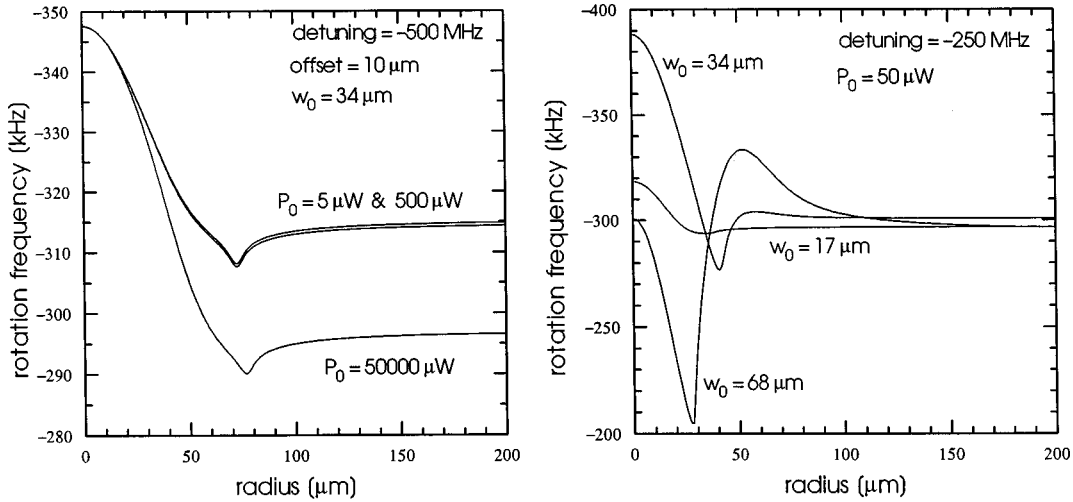
FIG. 20. Rotation frequency of an ion at equilibrium with the laser cooling beam as a function of the radius of its orbit.

laser cooled ion steady state using Eq. (27) gives reliable results.

F. Discussion

1. Axial and tilted crystals

We saw that the laser-cooled steady states are essentially laser power independent. Therefore, in the case of a Gaussian beam, as its width is independent of the position, a displacement of an ion in the z direction will not change the laser-cooled steady states. This means that the results obtained here can easily be extended to axial and tilted configurations of the two-ion crystal. The main difference will be the variability of the crystal orientation on the laser settings, with maybe the possibility of observing bistability between these configurations.

2. Experimental aspects

The forming of the two-ion crystal could be verified using an imaging system or the photon-photon correlation technique [11]. With an imaging system, no accurate information on the crystal rotation frequency can be easily obtained. For this, the photon-photon correlation technique would be much more appropriate. However, we saw that the crystal orbit, in phase space, tends to align along the lines of constant fluorescence, i.e., the crystal steady state corresponds to a minimum of the fluorescence modulation. As a consequence, only little modulation should be observed in the photon correlation distribution. This modulation is expected to be bigger for large crystal radii (small space-charge shift), and nearly zero for crystals at Brillouin flow. This would explain why only slightly space-charge-shifted oscillation frequencies have been observed on the photon correlation distribution whenever there was evidence that small crystals were formed [5,11].

IV. LASER COOLING OF LARGER CRYSTALS AND CLOUDS

For larger planar crystals consisting of a single ring of ions, the maps obtained for the two-ion crystal can readily be calculated. It turns out, not surprisingly, that these maps are nearly identical to the two-ion crystal maps, even for the case of six ions.

A. Maps and shear calculations for larger crystals

1. Shear calculations

Until now, we have only considered crystals made of a single ring of ions. When the crystal is made of several rings,
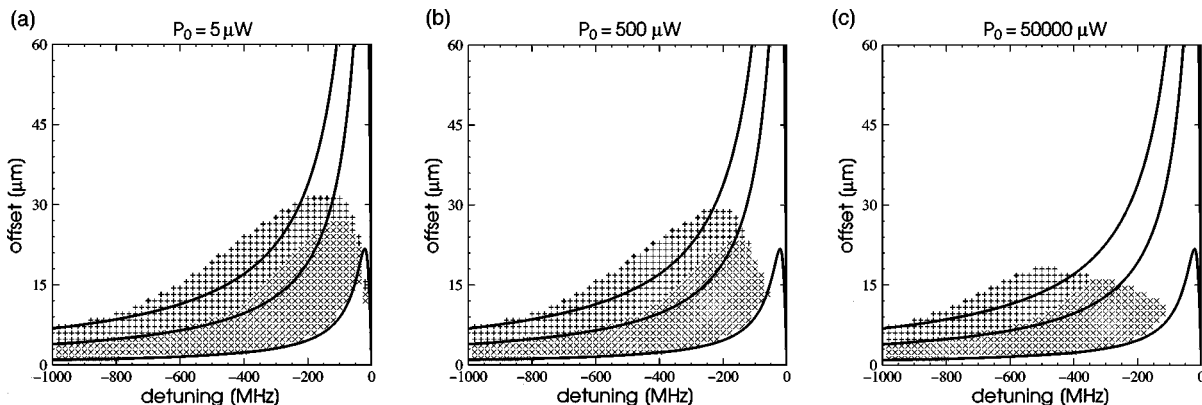

FIG. 21. Maps for two-ion crystals whose Coulomb repulsion has been artificially increased such that the ion's minimum separation is about 220 μm.
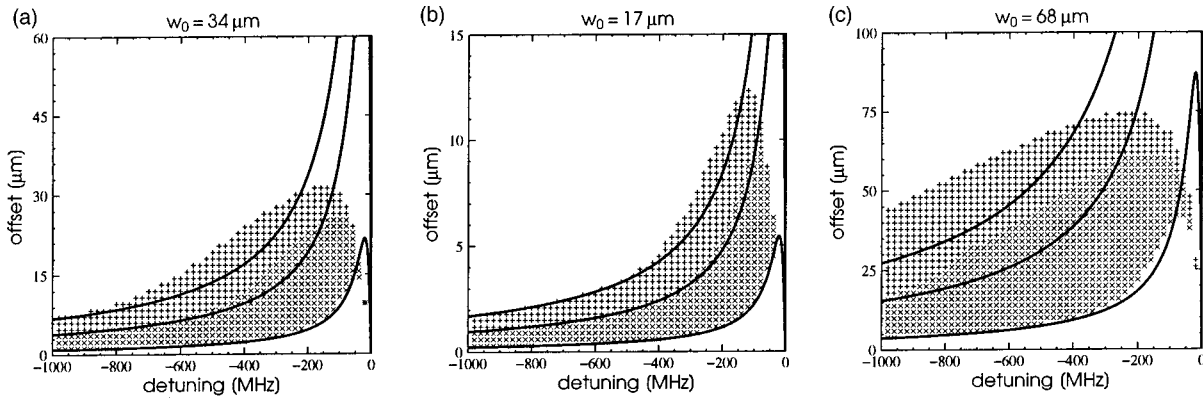
FIG. 22. Same as Fig. 21 but for various beam waists.

concentric and/or parallel, we can expect the laser-cooled steady state to be different for different rings. Concentric rings could have steady states dependent on their radii, while parallel rings (along the z axis) could have steady states dependent on the laser power. These steady states would differ by the rotation frequency of the rings; i.e., if we ignore any coupling between shells, we can expect the presence of shear, either in the radial plane or in the axial direction, or even both. We can easily calculate this shear using Eq. (30), where for a given value of the motion radius we can numerically calculate the rotation frequency ω_r (the ring rotation frequency) at which the circular motion is at equilibrium with the laser cooling. Figure 20 shows the result of this calculation for various laser powers and beam waists. For this last case, the laser detuning was set at -250 MHz, while the beam offset was adjusted for each beam waist such that for infinite radii the steady state is close to Brillouin flow. We see that we can expect to observe some relatively strong radial shear. This shear would be relatively small for small laser beams and relatively strong for large beams. We do expect the shear to depend on the beam waist size, but the fact that the shear magnitude increases with the beam waist is rather surprising. One would rather expect the shear magnitude to decrease with beam waist. A variation in laser power seems to have a much smaller effect on the shear. There seems to be a threshold value of laser power at which the change in shear becomes suddenly important. In practice, couplings between shells are likely to reduce or eliminate sheer [17].

2. Large crystal maps

There is another way to calculate numerically the steady state of a large cloud. This can be done by calculating the two-ion crystal steady-state maps but with an artificially increased Coulomb repulsion. Doing this increases the crystal minimum separation to values close to the radius of a large crystal. Figures 21 and 22 show such maps for various laser powers and beam waists, respectively. For those plots the Coulomb repulsion was increased such that at Brillouin flow the crystal separation is about 220 μm.

A number of features are common to all these maps. First, we see that for large detunings, the analytically calculated Brillouin flow line agrees well with the numerically calculated values. Second, the maximum possible laser offset for which the crystal can be ''cooled'' to Brillouin flow does

exceed the beam waist size. This maximum offset even decreases for larger laser powers. Third, the smallest possible detuning is in all cases larger than one linewidth; again, it is worse for larger laser powers. In fact, similarly to the ''normal'' two-ion crystal, we expect that for small laser detunings, a crystal set at Brillouin flow will not be stable.

Surprisingly, the cooling regions calculated numerically fit best the analytically calculated boundaries for smaller beam waists. We would rather expect the opposite, as the analytical boundaries are calculated in the limit of small radii. For large laser powers, the stability regions seem to be pushed away from resonance. This could be due to the power broadening of the resonance linewidth.

B. Discussion

Itano and Wineland showed that the minimum temperature for a single ion was obtained with a laser detuning of $-\Gamma/2$ [6]. In the case of the two-ion crystal, it was clear that the crystal temperature decreased as the resonance was approached, although the crystal became unstable before $-\Gamma/2$ was reached. By analogy, we can expect the same to be true of large clouds. However, we saw that large clouds at Brillouin flow are not stable for small detunings. From this point of view, we cannot expect to achieve very low temperatures in our clouds. It seems that the larger the cloud, the larger the smallest possible detuning. This means that the lowest achievable temperature would increase with the cloud size. However, crystallization of very large beryllium ion clouds has been observed [18], but this was achieved with the use of more than one laser beam: in this case, one beam was used to control the cloud rotation frequency, and the other beam was used to cool the cloud.

V. CONCLUSIONS

In this paper we have presented an approach, based on a phase-space picture, to the theory of laser cooling in the Penning trap. This phase-space picture proved to be very useful in helping to reduce the number of degrees of freedom involved. In the case of a single ion, considering small orbits, we were able to find an analytical expression for the conditions the laser offset and detuning must fulfill in order to simultaneously cool both magnetron and modified cyclotron degrees of freedom. Numerical calculations showed that this analytical result was a very good approximation even in the

case of larger magnetron or modified cyclotron radii. The presence of ''laser-trapped'' steady states of the motion was confirmed and their stability proved. The position of these states in laser detuning-offset space seems to fit well with experimental observations. The case where both magnetron and modified cyclotron radii are nonzero was also investigated numerically. In the limit of small radii, the analytical result was retrieved. For larger radii, some unexpected features, such as the possibility, in some cases, of cooling both degrees of freedom with a *positive* laser detuning and a *negative* offset, were observed. The phase-space picture provided us with the means of explaining these results. Although these results were obtained in the case were the laser beam is directed parallel to the trap radial plane, it was shown that most results obtained were still qualitatively valid in the case of a beam set at an angle with respect to the radial plane. These results allowed us to propose a ''recipe'' for the cooling of a single ion. This should prove to be very useful for future experiments requiring the trapping and laser cooling of single ions. Furthermore, these results could also be used to determine the laser offset to a very high precision.

The same phase-space picture was used to study the laser cooling of the two-ion crystal. It was shown that, seen from this phase space, the crystal rotation frequency ''locks'' to the ion's fluorescence contour lines. Interestingly, it was found that the regions in laser detuning-offset space where the two-ion crystal is cooled are essentially identical to the small radii single-ion case. This provided us with an analytical expression for the condition in laser detuning and offset for which the two-ion crystal is at Brillouin flow. This result was shown to fit perfectly the numerical results for laser detunings larger than one resonance linewidth. An extension of this calculation provided us with an analytical expression for the crystal rotation frequency or separation as a function of the laser detuning and offset. These results could relatively easily be verified experimentally. We saw that the photon-photon correlation technique [11] for measuring the crystal rotation frequency might not always provide us with adequate data, as at equilibrium the modulation of the scattered light by the ions is minimized. However, using narrower laser beams might help in increasing the fluorescence modulation, although this would require extremely accurate beam positioning. Alternatively, the use of a second laser beam oriented along the *z* axis, so as not to disturb the perpendicular laser cooling, could also increase the fluorescence modulation. An interesting application which could make use of small planar ion crystals is the measurement of the expected azimuthal Doppler shift and light radiation torque one can expect from Laguerre-Gaussian beams [19,20].

ACKNOWLEDGMENTS

[1] D. J. Wineland and H. G. Dehmelt, Bull. Am. Phys. Soc. **20**, 637 (1975).

[2] T. W. Hänsch and A. C. Schawlow, Opt. Commun. **13**, 68 (1975).

[3] D. J. Wineland, R. E. Drullinger, and F. L. Walls, Phys. Rev. Lett. **40**, 1639 (1978).

[4] R. C. Thompson, Phys. Scr. **25**, 318 (1988).

[5] D. C. Wilson, Ph.D. thesis, Imperial College, London, 1992 (unpublished).

[6] W. M. Itano and D. J. Wineland, Phys. Rev. A **25**, 35 (1982).

[7] W. M. Itano, L. R. Brewer, D. J. Larson, and D. J. Wineland, Phys. Rev. A **38**, 5698 (1988).

[8] M. Kretschmar, Eur. J. Phys. **12**, 240 (1991).

[9] J. Byrne and P. S. Farago, Proc. Phys. Soc. London **86**, 801 (1965); H. Dehmelt, Adv. At. Mol. Phys. **3**, 53 (1967); **5**, 109 (1969).

[10] A. Yariv, *Quantum Electronics* (Wiley, New York, 1989).

[11] K. Dholakia, G. Z. K. Horvath, D. M. Segal, R. C. Thompson, D. M. Warrington, and D. C. Wilson, Phys. Rev. A **47**, 441 (1993).

[12] J. Hoffnagle and R. G. Brewer, Phys. Rev. Lett. **71**, 1828 (1993).

[13] D. Farrelly and J. E. Howard, Phys. Rev. A **49**, 1494 (1994).

[14] R. C. Thompson and D. C. Wilson, Z. Phys. D **42**, 271 (1997).

[15] G. Zs. K. Horvath, Ph.D. thesis, Imperial College, London, 1995 (unpublished).

[16] G. Zs. K. Horvath and R. C. Thompson (unpublished).

[17] S. L. Gilbert, J. J. Bollinger, and D. J. Wineland, Phys. Rev. Lett. **60**, 2022 (1988).

[18] J. N. Tan, J. J. Bollinger, B. Jelenkovic, and D. J. Wineland, Phys. Rev. Lett. **75**, 4198 (1995).

[19] L. Allen, M. W. Beijersbergen, R. J. C. Spreeuw, and J. P. Woerdman, Phys. Rev. A **45**, 8185 (1992).

[20] W. Power and R. C. Thompson, Opt. Commun. **132**, 371 (1996).